Published in final edited form as:
Am J Ophthalmol. 2008 July ; 146(1): 121–127. doi:10.1016/j.ajo.2008.03.001.

Ultrastructural Correlation of Spectral-Domain Optical Coherence Tomographic Findings in Vitreomacular Traction Syndrome

LOUIS K. CHANG, **HOWARD F. FINE**, **RICHARD F. SPAIDE**, **HIDEKI KOIZUMI**, and **HANS E. GROSSNIKLAUS**
Vitreous-Retina-Macula Consultants of New York, and the LuEsther T. Mertz Retinal Research Center, Manhattan Eye, Ear, and Throat Hospital, New York, New York (L.K.C., H.F.F., R.F.S., H.K.); and the L. F. Montgomery Ophthalmic Pathology Laboratory, Emory University, Atlanta, Georgia (H.E.G.)

Abstract

PURPOSE—To examine the ultrastructural correlates of spectral-domain optical coherence tomography (SD-OCT) findings in patients with vitreomacular traction (VMT).

DESIGN—Observational case series.

METHODS—Retrospective analysis of six eyes of consecutive patients who underwent vitrectomy surgery for VMT was performed in this single-center, noncomparative study. One patient had a concurrent macular hole. Preoperative assessment included SD-OCT examination with 3-dimensional image reconstruction. During surgery the vitreous cone was dissected from the vitreous body using scissors, then removed from the surface of the retina with a combination of sharp dissection and peeling, and subsequently submitted for histologic and transmission electron microscopic processing.

RESULTS—SD-OCT showed prominent vitreal-foveal adhesion in all six eyes. Each eye had an epiretinal membrane (ERM) under the detached perifoveal posterior vitreous detachment. In all eyes this ERM appeared to course up the cone of attached vitreous and along the back surface of the posterior vitreous face. Ultrastructural analysis showed fibrocellular proliferations in the vitreous specimens in all six cases, which included retinal pigment epithelium (RPE) cells (five eyes), fibrocytes (four eyes), and macrophages (three eyes).

CONCLUSIONS—The adhesion between the vitreous and fovea in vitreomacular traction syndrome is accompanied by fibrocellular proliferation along the exposed surfaces of the inner retina and the posterior surface of the vitreous. This fibrocellular proliferation may augment the adhesion between the vitreous and fovea, and may account for the prominent OCT signal seen along the posterior surface of the vitreous in these cases.

Vitreomacular traction (VMT) syndrome results from persistent vitreoretinal adhesions in the setting of partial posterior vitreous detachment (PVD). The vitreoretinal adhesions transmit tractional forces to the retina from the vitreous body, having the potential to cause tensile deformation, foveal cavitation, cystoid macular edema, limited macular detachment, or macular hole (MH) formation.[1,2] Our understanding of VMT has been enhanced by the development of optical coherence tomography (OCT), a noninvasive method of imaging intraocular tissues.[3–11]

Inquiries to Richard F. Spaide, Vitreous, Retina, Macula Consultants of New York, 460 Park Avenue, 5th Floor, New York, NY 10022; rickspaide@yahoo.com.

Idiopathic epiretinal membrane (ERM) proliferation is another vitreoretinal interface abnormality that is often considered to be distinct from VMT.[1] Astrocytes, myofibroblasts, and fibrocytes predominate in VMT[1,11–14] while retinal pigment epithelium (RPE) cells are commonly found in ERMs.[2,15–18] However, a recent study with spectral-domain (SD) OCT showed similarities between the anatomic features of these two entities.[19] In the current study, we performed preoperative SD-OCT and transmission electron microscopy (TEM) of surgically excised specimens from patients with VMT to further define the relationship between imaging and the pathologic findings in this condition.

METHODS

Six eyes of six consecutive patients who underwent pars plana vitrectomy with membrane peeling for VMT were included in this retrospective study. All patients were seen at a single, referral-based retina practice. Each eye underwent complete preoperative ophthalmic examination including best-corrected Snellen visual acuity (VA), biomicroscopy, color fundus photography, and SD-OCT analysis (3D OCT 1000 version 2.00; Topcon Corp, Paramus, New Jersey, USA). This SD-OCT system used in this study employs a superluminescent diode with a center wavelength of 830 nm and bandwidth of 50 nm as a light source. The system acquires 128 horizontal B-scan images, each containing 512 A-scans, covering a 6 mm horizontal × 6 mm vertical × 1.7 mm axial volume in less than 3.7 seconds. Using this raster scan protocol, the horizontal pixel spacing was 11 μm (6 mm/512) and the vertical spacing was 47 μm (6 mm/128). After the completion of the scan, a color fundus photograph is taken with an integrated nonmydriatic camera. The B-scan images can be used to form a monochromatic projection image of the fundus that has point-to-point registration with any A-scan. The B-scans within the 6 × 6-mm block can be used to construct 3-dimensional (3D) images, which provide improved visualization of spatial relationships of vitreoretinal structures. The sizes of the horizontal and vertical axes of the vitreous attachment were measured from the raster scan protocol centered on the fovea of each patient. The vitreoretinal adhesion was considered focal if the greatest diameter of vitreoretinal adhesion was less than 1500 microns and broad if greater than 1500.[19]

Patients underwent pars plana vitrectomy with membrane removal by a single surgeon (R.F.S.) using 23-gauge instrumentation (Dutch Ophthalmic USA, Exeter, New Hampshire, USA) and an Alcon Accurus vitrectomy system (Alcon Laboratories Inc, Fort Worth, Texas, USA).[20] After core vitrectomy, the vitreous cone surrounding the area of macular traction was released from the remainder of the posterior hyaloid face using scissors dissection. The attachment between the vitreous and fovea was separated by a combination of sharp dissection and peeling. The specimen was collected by manually aspirating it in through the vitrector tip into a 3 ml syringe by using a three-way stopcock. The specimen was transferred into a vial of 4% glutaraldehyde for TEM processing. In one case (Case 6), trypan blue was used to stain a residual ERM adjacent to the area of VMT that remained after the vitreous cone was removed. This membrane was peeled, harvested separately, fixed in 4% glutaraldehyde, and processed. This patient also had a full-thickness MH, so 20% sulfur hexafluoride gas tamponade with prone positioning was used in this case. The Snellen VA was converted to the logarithm of the minimal angle of resolution (logMAR) prior to descriptive statistical analysis.

ULTRASTRUCTURAL ANALYSIS

The surgically excised specimens were submitted in 4% glutaraldehyde and processed for TEM. The specimens were postfixed with 0.1 mol/l of cacodylate buffer and 1% osmium tetroxide. After standard dehydration, the specimens were embedded in epoxy resin and semithin (0.1-μm) sections were cut and stained with toluidine blue. Thin sections were then cut and stained with uranyl acetate–lead citrate. Previously published criteria were used to

identify specific cell types such as the RPE, vascular endothelium, fibrocytes, myofibroblasts, glial cells, photoreceptors, macrophages, and lymphocytes and also extracellular components, including collagen.[21]

RESULTS

The mean age of the patients was 75.2 years (range, 65 to 82; Table). Two of the patients were male, four were female. The mean preoperative VA was 20/78 (logMAR 0.59; range, 20/40 to 20/200). There were no intraoperative surgical complications. The mean postoperative VA was 20/54 (logMAR 0.43; range, 20/30 to 20/100) with an average follow-up of 32 weeks (range, 1.5 to 95 weeks).

SPECTRAL-DOMAIN OPTICAL COHERENCE TOMOGRAPHIC FINDINGS

Preoperative SD-OCT demonstrated partial PVD with persistent vitreoretinal adhesions involving the fovea in all six cases (Figures 1 and 2). VMT was focal in four cases and broad in two cases. Among those with focal VMT, three had foveal cavitation and one had a full-thickness MH. Of the two cases with broad-based VMT, one had cystoid macular edema and one had diffuse retinal thickening without pseudocyst formation. A hyperreflective linear signal on the surface of the macula, consistent with an ERM, was observed in all patients. Contiguous with this ERM was a continuation of increased reflectivity that coursed up along the back surface of the detached posterior vitreous.[19] The casing of increased reflectivity on the vitreous face could be best seen with the 3D reconstructions. The membranous structure on the vitreous face was about 10 to 20 μm thick and continued along the expanding convexity of the posterior hyaloid face for varying distances. The outer edge of the membranous thickening along the posterior vitreous face was well defined.

TRANSMISSION ELECTRON MICROSCOPIC FINDINGS

Ultrastructural analysis showed a fibrocellular proliferation in the vitreous specimens in all six cases. Collagen fibrils that measured between 9 and 12 nanometers in diameter were seen in all specimens. A variety of cell types were seen in association with the collagen, including RPE (n = 5, Figures 2, 3, 4, and 6), macrophages (n = 3, Figures 3 and 4), myofibroblasts (n = 1), fibrocytes (n = 3, Figures 2 and 5), and hyalocytes (n = 1). Internal limiting membrane (ILM) was observed in three specimens, associated in all cases with collagen fibrils. In Case 5, collagen was interposed between ILM and fibrocytes. In Case 6, the ERM was composed of RPE cells with a layer of collagen fibrils sandwiched between the ERM and the ILM (Figure 6). There appeared to be a layer of protein deposited under the proliferating cells that may represent basement membrane and extracellular matrix formation (Figure 2).

DISCUSSION

In this study, we evaluated patients with prominent vitreomacular traction with SD-OCT and then examined the corresponding vitreous specimen with TEM. By SD-OCT with 3D reconstruction we found the expected cone of vitreous with persistent attachment to the central macula. The eyes had findings consistent with ERM formation in areas of PVD. In addition, the membrane appeared to course up the vitreous cone and formed a hyperreflective encasement of the posterior portion of the persistent vitreous attachment. Corresponding TEM of the vitreous specimens identified cells ordinarily found in ERMs proliferating on the posterior vitreous cortex.

The OCT appearance of the vitreous varies substantially in reflectivity. In 2-dimensional representations there can be thickening and hyperreflectivity of the posterior vitreous face adjacent to regions where the reflectivity from the vitreous face is quite low. This variation in

reflectivity was used to generate a grading system for a pre–MH state known as "stage 0" MHs.[22] The severity of stage 0 MHs was graded as mild, moderate, and severe based on the amount and distribution of reflectivity from the posterior vitreous immediately adjacent to the site of vitreoretinal attachment.[22] Stage 0 MHs appear to correspond to what we have termed focal vitreomacular traction,[19] with the increased reflectivity from the posterior vitreous face accounted for by cellular proliferation as demonstrated in the present article.

We observed several types of cells not usually present in the vitreous cavity, including RPE cells, myofibroblasts, and fibrocytes. Most striking was the presence of RPE cells in five of six vitreous specimens, a typical feature of ERMs.[15–18] This is in contrast to previous histologic studies of vitreomacular traction that found predominately myofibroblasts, fibrocytes, fibrous astrocytes, and an absence of RPE cells.[11–14] However the previous studies examined specimens removed from the surface of the retina at the site of vitreoretinal attachment and did not concentrate on the vitreous cone above the retina as we did.

The ERM and the ILM specimens removed showed native collagen sandwiched between the ILM and RPE cells. A PVD appears to form by a splitting within the vitreous cortex, leaving remnants of vitreous on the foveal surface.[23] The vitreous cortex remains on the ILM surface and appears to act as scaffolding for cellular proliferation (Figure 7). The corresponding side of the split vitreous cortex forms the outer surface of the cone of detached vitreous. This portion of the vitreous cortex appears to be able to act as scaffolding for the proliferation of cells as well. The proliferating cells and their associated extracellular matrix may fortify the attachment strength of the vitreoretinal adhesion to the fovea, helping to prevent the ordinarily expected complete separation of the vitreous from the macular surface. A wound-healing response may be the underlying reason for the cellular proliferation.

The origin of the cells comprising ERMs, and in these cases the proliferation along the back surface of the vitreous cone, is unknown. We and others relied exclusively on morphologic criteria to identify cell types in the ultrastructural analysis.[11–14] A weakness of this approach is the variation in appearance of the observed cells. One of our patients had a MH, offering a route of access for the observed RPE cells. However, the other cases had no retinal breaks, but they still had proliferation of glial and RPE cells. Small mechanical defects in the ILM have been proposed as the means of access for proliferating cells, but this defect would not seem to directly explain the presence of RPE cells. It is not known if a mechanical defect of the ILM is a necessary requisite for the passage of these cells in the first place.

Vinores and associates performed immunocytochemical analysis on idiopathic ERM specimens and found that cells that had typical morphologic features of RPE cells did not necessarily express the expected profile of antigens.[24] RPE cells have been shown to undergo epithelial-to-mesenchymal transition in vitro, with changes in epithelial cell markers,[25] which is one possible explanation for this occurrence. Another interesting possibility involves bone marrow–derived progenitor cells. Approximately half of the proliferating cells in experimental choroidal neovascularization are derived from bone marrow–derived progenitor cells.[26] Bone marrow–derived progenitor cells home to corneal alkali injuries and promote wound healing.[27] Following RPE injury bone marrow–derived cells migrate into the eye and adopt RPE characteristics.[28–31] This raises the possibility that cells seen proliferating along the surface of the retina and along the back surface of the vitreous cone may also have originated, in part, from bone marrow–derived progenitor cells.

Our SD-OCT and TEM data demonstrate ERM formation in the setting of VMT. Our ultrastructural analysis suggests that these eyes have a fibrocellular proliferation on the posterior vitreous surface with composition similar to idiopathic ERM on the retinal surface.

The fibrocellular proliferation along the retinal and vitreal interfaces in VMT may both contribute to the tenacity of vitreoretinal adhesion in seen in this condition.

Acknowledgments

This study was supported in part by the heed ophthalmic foundation, cleveland, ohio (drs chang and fine) and the Macula Foundation (Dr Spaide), New York, New York. Drs Koizumi and Spaide have received consulting fees from Topcon Medical Systems, Paramus, New Jersey. Involved in design and conduct of study (L.K.C., H.F.F., R.F.S., H.K.); collection, management, analysis, and interpretation of the data (L.K.C., H.F.F., R.F.S., H.K., H.E.G.); and preparation, review, and approval of the manuscript (L.K.C., H.F.F., R.F.S., H.K., H.E.G.). Institutional Review Board (IRB) approval of Western IRB was obtained for this study. The study protocol adhered to tenets of the Declaration of Helsinki and was HIPAA compliant.

References

1. Smiddy WE, Michels RG, Green WR. Morphology, pathology, and surgery of idiopathic vitreoretinal macular disorders: a review. Retina 1990;10:288–296. [PubMed: 2089546]
2. Johnson MW. Perifoveal vitreous detachment and its macular complications. Trans Am Ophthalmol Soc 2005;103:537–567. [PubMed: 17057817]
3. Gallemore RP, Jumper JM, McCuen BW II, et al. Diagnosis of vitreoretinal adhesions in macular disease with optical coherence tomography. Retina 2000;20:115–120. [PubMed: 10783942]
4. Uchino E, Uemura A, Doi N, Ohba N. Postsurgical evaluation of idiopathic vitreomacular traction syndrome by optical coherence tomography. Am J Ophthalmol 2001;132:122–123. [PubMed: 11438072]
5. Larsson J. Vitrectomy in vitreomacular traction syndrome evaluated by ocular coherence tomography (OCT) retinal mapping. Acta Ophthalmol Scand 2004;82:691–694. [PubMed: 15606465]
6. Yamada N, Kishi S. Tomographic features and surgical outcomes of vitreomacular traction syndrome. Am J Ophthalmol 2005;139:112–117. [PubMed: 15652835]
7. Johnson MW. Tractional cystoid macular edema: a subtle variant of the vitreomacular traction syndrome. Am J Ophthalmol 2005;140:184–192. [PubMed: 16086944]
8. Forte R, Pascotto F, de Crecchio G. Visualization of vitreomacular tractions with en face optical coherence tomography. Eye 2007;11:1391–1394. [PubMed: 16751756]
9. Ito Y, Terasaki H, Mori M, et al. Three-dimensional optical coherence tomography of vitreomacular traction syndrome before and after vitrectomy. Retina 2000;20:403–405. [PubMed: 10950422]
10. Do DV, Cho M, Nguyen QD, et al. Impact of optical coherence tomography on surgical decision making for epiretinal membranes and vitreomacular traction. Retina 2007;27:552–556. [PubMed: 17558315]
11. Gandorfer A, Rohleder M, Kampik A. Epiretinal pathology of vitreomacular traction syndrome. Br J Ophthalmol 2002;86:902–909. [PubMed: 12140213]
12. Gastaud P, Betis F, Rouhette H, Hofman P. Ultrastructural findings of epimacular membrane and detached posterior hyaloid in vitreomacular traction syndrome. J Fr Ophtalmol 2000;23:587–593. [PubMed: 10880925]
13. Smiddy WE, Green WR, Michels RG, de la Cruz Z. Ultra-structural studies of vitreomacular traction syndrome. Am J Ophthalmol 1989;107:177–185. [PubMed: 2913812]
14. Shinoda K, Hirakata A, Hida T, et al. Ultrastructural and immunohistochemical findings in five patients with vitreomacular traction syndrome. Retina 2000;20:289–293. [PubMed: 10872935]
15. Smiddy WE, Maguire AM, Green WR, et al. Idiopathic epiretinal membranes. Ultrastructural characteristics and clinicopathologic correlation. Ophthalmology 1989;96:811–820. [PubMed: 2740079]
16. Heilskov TW, Massicotte SJ, Folk JC. Epiretinal macular membranes in eyes with attached posterior cortical vitreous. Retina 1996;16:279–284. [PubMed: 8865386]
17. Kampik A, Kenyon KR, Michels RG, et al. Epiretinal and vitreous membranes. Comparative study of 56 cases. Arch Ophthalmol 1981;99:1445–1454. [PubMed: 7020665]
18. Clarkson JG, Green WR, Massof D. A histopathological review of 168 cases of preretinal membrane. Am J Ophthalmol 1977;84:1–17. [PubMed: 900209]

19. Koizumi H, Spaide RF, Fisher YL, et al. Three-dimensional evaluation of vitreomacular traction and epiretinal membrane using spectral-domain optical coherence tomography. Am J Ophthalmol 2008;145:509–517. [PubMed: 18191099]

20. Fine HF, Iranmanesh R, Iturralde D, Spaide RF. Outcomes of 77 consecutive cases of 23-gauge transconjunctival vitrectomy surgery for posterior segment disease. Ophthalmology 2007;114:1197–1200. [PubMed: 17544779]

21. Green, WR. The retina. In: Spencer, WH., editor. Ophthalmic pathology: An atlas and textbook. Philadelphia, Pennsylvania: WB Saunders Co; 1996. p. 982-1051.

22. Chan A, Duker JS, Schuman JS, Fujimoto JG. Stage 0 macular holes: observations by optical coherence tomography. Ophthalmology 2004;111:2027–2032. [PubMed: 15522368]

23. Kishi S, Demaria C, Shimizu K. Vitreous cortex remnants at the fovea after spontaneous vitreous detachment. Int Ophthalmol 1986;9:253–260. [PubMed: 3793377]

24. Vinores SA, Campochiaro PA, Conway BP. Ultrastructural and electron-immunocytochemical characterization of cells in epiretinal membranes. Invest Ophthalmol Vis Sci 1990;31:14–28. [PubMed: 1688833]

25. Grisanti S, Guidry C. Transdifferentiation of retinal pigment epithelial cells from epithelial to mesenchymal phenotype. Invest Ophthalmol Vis Sci 1995;36:391–405. [PubMed: 7531185]

26. Espinosa-Heidmann DG, Caicedo A, Hernandez EP, et al. Bone marrow–derived progenitor cells contribute to experimental choroidal neovascularization. Invest Ophthalmol Vis Sci 2003;44:4914–4919. [PubMed: 14578417]

27. Ye J, Lee SY, Kook KH, Yao K. Bone marrow–derived progenitor cells promote corneal wound healing following alkali injury. Graefes Arch Clin Exp Ophthalmol 2008;246:217–222. [PubMed: 18075751]

28. Harris JR, Brown GA, Jorgensen M, et al. Bone marrow–derived cells home to and regenerate retinal pigment epithelium after injury. Invest Ophthalmol Vis Sci 2006;47:2108–2113. [PubMed: 16639022]

29. Atmaca-Sonmez P, Li Y, Yamauchi Y, et al. Systemically transferred hematopoietic stem cells home to the subretinal space and express RPE-65 in a mouse model of retinal pigment epithelium damage. Exp Eye Res 2006;83:1295–1302. [PubMed: 16949576]

30. Li Y, Reca RG, Atmaca-Sonmez P, et al. Retinal pigment epithelium damage enhances expression of chemoattractants and migration of bone marrow–derived stem cells. Invest Ophthalmol Vis Sci 2006;47:1646–1652. [PubMed: 16565405]

31. Li Y, Atmaca-Sonmez P, Schanie CL, et al. Endogenous bone marrow–derived cells express retinal pigment epithelium cell markers and migrate to focal areas of RPE damage. Invest Ophthalmol Vis Sci 2007;48:4321–4327. [PubMed: 17724223]

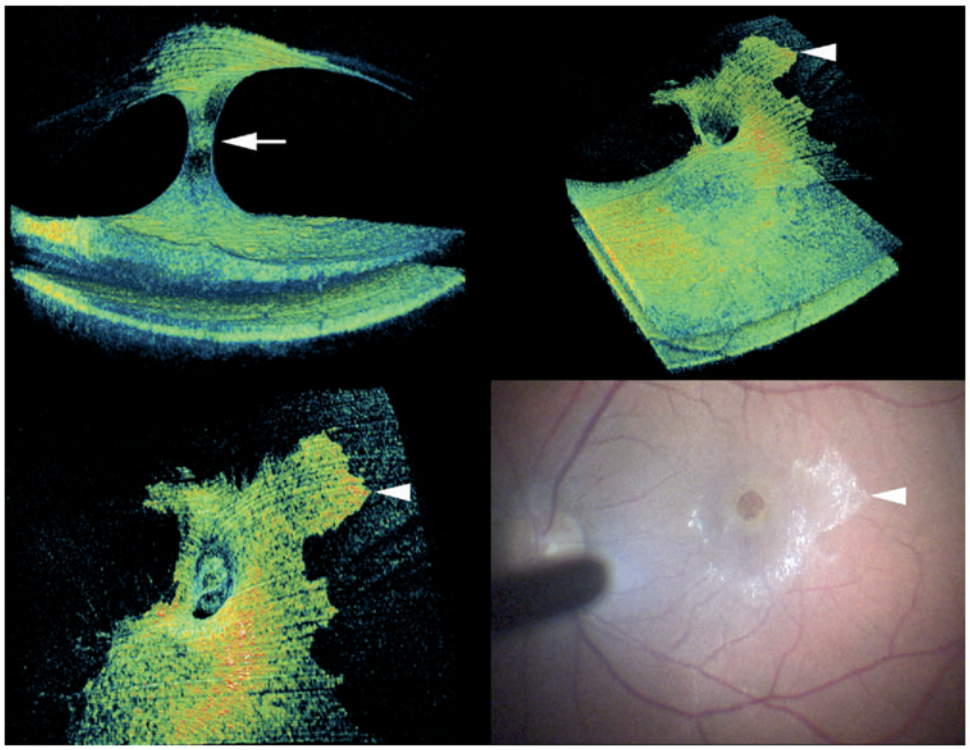

FIGURE 1.

Patient 6 with vitreomacular traction (VMT) with associated epiretinal membrane (ERM) and macular hole. Preoperative 3-dimensional (3D) spectral-domain optical coherence tomography (SD-OCT) shows cone-shaped vitreoretinal adhesion (arrow, Top left) and a prominent ERM on retinal surface (Top right) with apparent continuation of this proliferation on the detached posterior hyaloid face (Top right and Bottom left). Note the clear distinction between the hyperreflective proliferation and the adjacent normal posterior hyaloid face. The proliferation on the posterior hyaloid was clearly visible intraoperatively (Bottom right). Arrowheads in Top right, Bottom left, and Bottom right panels mark identical location on the proliferation on the posterior vitreous.

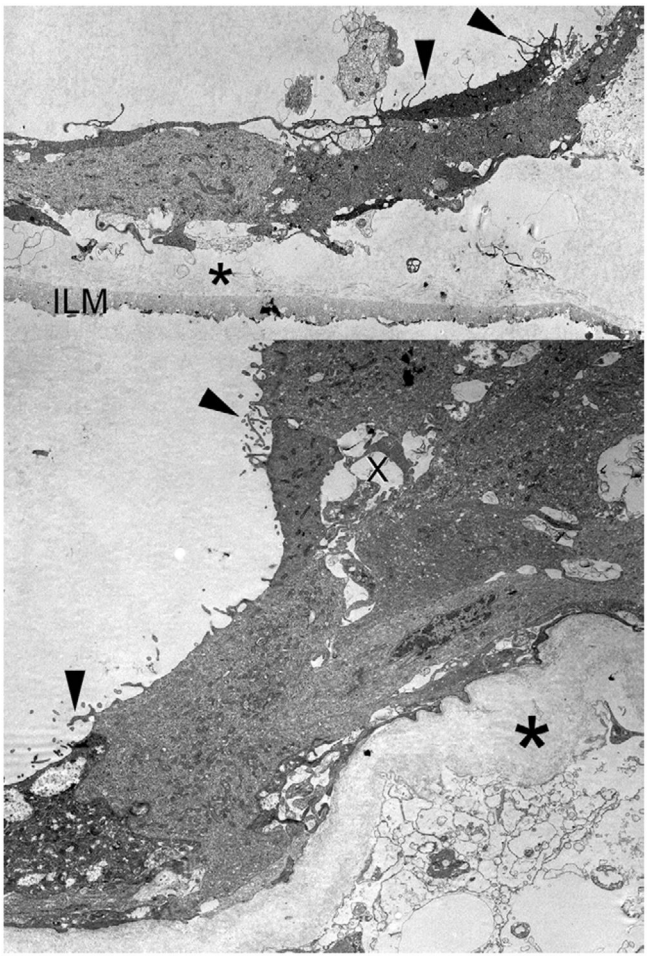

FIGURE 2.

Ultrastructural analysis of ERM in vitreous cone of Patient 6 with vitreous (10 to 12 nm) collagen (asterisk), which is sandwiched between retinal pigment epithelium (RPE) with surface mircovilli (arrowheads) and internal limiting membrane (ILM, Top). Higher magnification of RPE cells shows microvillous processes (arrowheads) forming tubuloacinar structures with lumens (x) and overlying posterior hyaloid 10- to 12-nanometer collagen fibrils (asterisk).

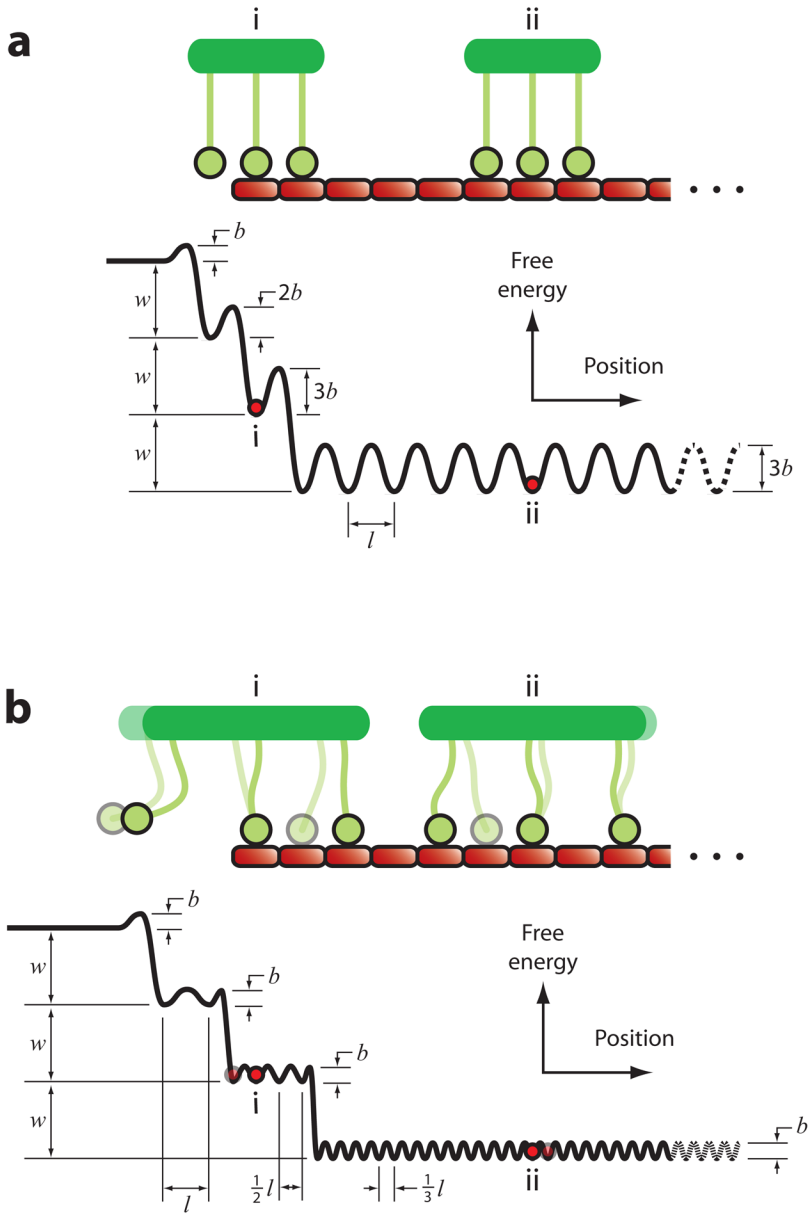

FIGURE 3.

Ultrastructural analysis of the specimen from Patient 4 with VMT. Transmission electron microscopy (TEM) of the membrane on the posterior vitreous with RPE cell forming acinar structures with lumens (x), vitreous collagen fibrils (asterisk), and a macrophage [M] (arrow).

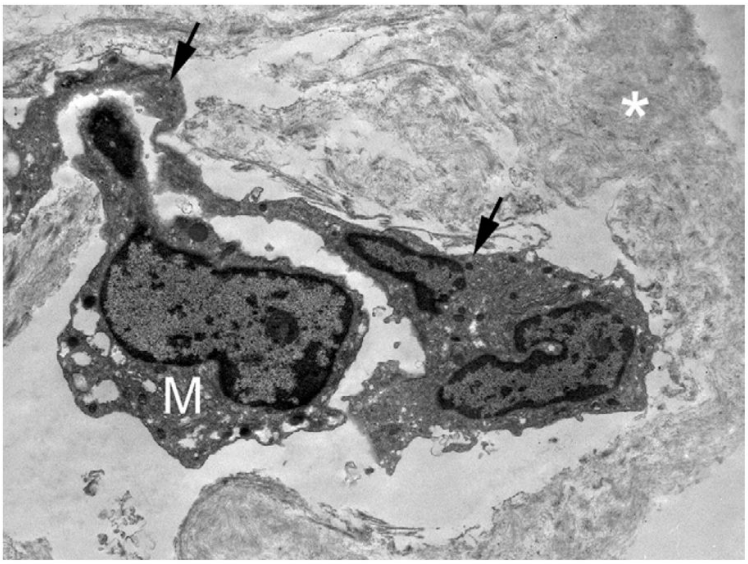

FIGURE 4.
TEM analysis of fibrocellular proliferation in Patient 5 showing an RPE cell (arrows) on collagen fibrils (asterisk) with an overlying M.

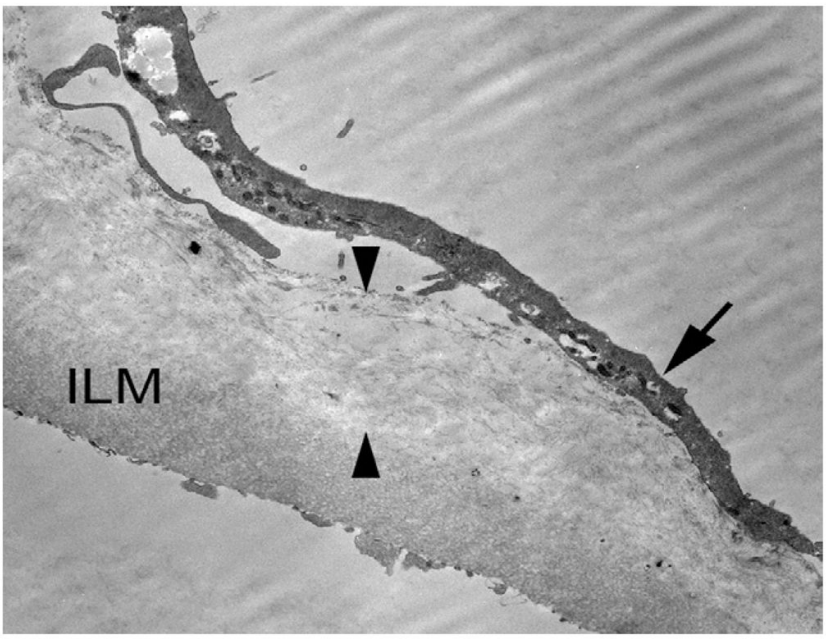

FIGURE 5.
ERM associated with VMT in Patient 5 consisting of a layer of 10-nm collagen fibrils (between arrowheads), which is interposed between the ILM and a layer of fibrocytes (arrow).

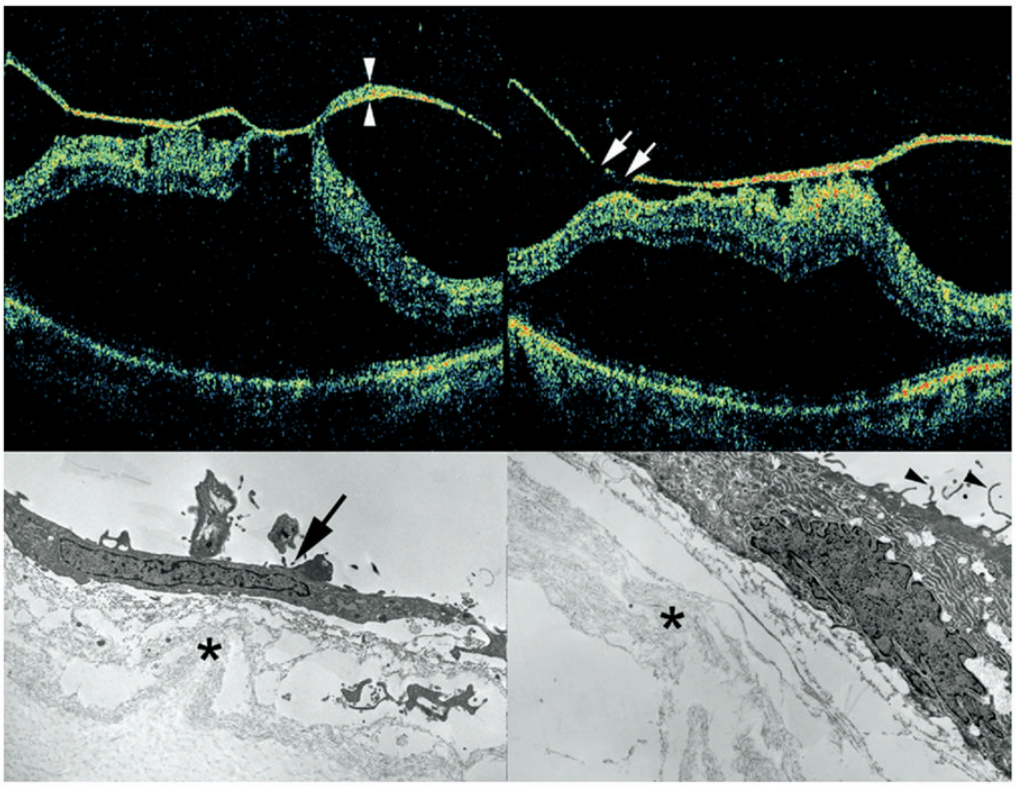

FIGURE 6.

SD-OCT and TEM findings in Patient 3 with VMT and ERM. Preoperative SD-OCT shows broad vitreomacular adhesion with retinal distortion and macular detachment (Top left and Top right). Note thickening and hyperreflectivity of the posterior hyaloid face. Skip areas in this hyperreflectivity (arrows, Top right) suggest that this signal represents abnormal fibrocellular proliferation on the posterior vitreous face, since the posterior hyaloid should be intact and continuous. TEM analysis of the surgical specimen from this same patient showed the membrane on the posterior hyaloid containing a fibrocyte (arrow) with abundant intracytoplasmic rough endoplasmic reticulum and cortical vitreous collagen fibrils (asterisk, Bottom left) and RPE cell with surface microvillus processes (arrowhead) and collagen fibrils (asterisk, Bottom right). Material between collagen fibrils and cellular elements likely represents extracellular matrix elaborated by neighboring cells.

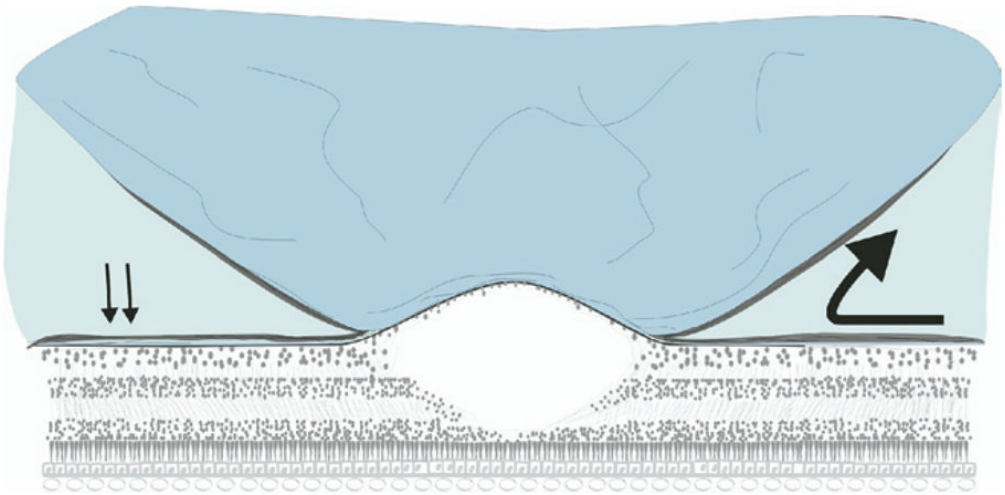

FIGURE 7.

Proposed mechanism of ERM proliferation in VMT syndrome. After partial posterior vitreous detachment with persistent vitreofoveal attachment, vitreous collagen remaining on the retina acts as a scaffolding for ERM formation (arrows). Fibrocellular proliferation continues past the vitreo-retinal interface onto the detached posterior hyaloid face (large arrow).

TABLE

Summary of Spectral-Domain Optical Coherence Tomography and Transmission Electron Microscopy Characteristics of the Cases of Vitreomacular Traction Syndrome

					SD-OCT Findings		TEM Findings							
	Age	**Preoperative VA**	**Postoperative VA**	**Follow-up (weeks)**	**VR Adhesion**	**Intraretinal Changes**	**ERM**	**ILM**	**RPE**	**MP**	**MF**	**FC**	**HC**	**Collagen Diameter**
1	65	20/60	20/40	95	Focal	Pseudocyst	+	−	+	−	+	−	−	9–10 nm
2	75	20/80	20/80	28	Focal	Pseudocyst	+	+	−	−	−	+	−	10 nm
3	78	20/100	20/100*	34	Broad	Diffuse thickening	+	−	+	+	−	+	−	10 nm
4	81	20/60	20/50	27	Focal	Pseudocyst	+	−	+	+	−	−	−	10 nm
5	82	20/40	20/40	1.5	Broad	Cystic edema	+	+	+	+	−	+	+	10 nm
6	70	20/200	20/40	2.7	Focal	Cystic edema and FTMH	+	+	+	−	−	−	−	10–12 nm

ERM = epiretinal membrane; FC = fibrocyte; FTMH = full-thickness macular hole; HC = hyalocytes; ILM = internal limiting membrane; MF = myofibrocyte; MP = macrophage; RPE = retinal pigment epithelium; SD-OCT = spectral-domain optical coherence tomography; TEM = transmission electron microscopy; VA = visual acuity; VR = vitreoretinal.

*This patient developed nuclear sclerosis and had a potential acuity measurement of 20/50.